Cl contents of phosphatic layers in First Phosphate's Bégin-Lamarche property, Quebec, Canada

Dr. Sandeep Banerjee,

Queen's University, Ontario, Canada

Respectfully submitted on November 10, 2023

Plain Language Summary

This report provides the results of analyses of the chlorine concentrations of fluorapatite ($Ca_5(PO_4)_3F$) crystals in potentially economic phosphatic layers from First Phosphate Corporation's Bégin-Lamarche property, Quebec, Canada. First Phosphate provided 28 drill core samples from 9 drill holes.

Samples were first studied with a petrographic microscope to identify the rock-forming minerals. More detailed mineralogic investigations were performed using a scanning electron microscope equipped with mineral liberation analysis to map the spatial relationship of minerals. Electron probe microanalysis provided chemical data for individual minerals.

Results indicate that fluorapatite composing phosphatic layers is hosted in peridotite (olivine + orthopyroxene + clinopyroxene + plagioclase + fluorapatite + magnetite + ilmenite), which is more specifically an olivine gabbronorite. In areas that are faulted, associated rocks contain ~700-10000 ppm Cl, reflecting alteration by Cl-enriched fluids during deformation. However, the Cl concentration of individual fluorapatite crystals is generally <700 ppm but can be as high as ~850 ppm.

The major conclusions of the study are:

1. The Cl content of apatite crystals (≤703 ppm with one sample of 863 ppm) from a limited number of samples (n=8) suggests that the Cl contents of apatite or phosphatic cumulate layers of the deposit are low.
2. Whole-rock Cl content is not related to the Cl content of individual apatite crystals within the peridotite. The highest measured Cl concentration in apatite (863 ppm) is reported from a sample with low whole-rock Cl content.
3. The Cl-enriched alteration minerals are iddingsite, and serpentine, which are associated with altered olivine and cross-cutting (serpentine) veins. This mineral assemblage was produced by the interaction with late-stage Cl-rich fluids and is responsible for the anomalously high Cl contents of some phosphatic cumulate layers.
4. The timing of the evolution of these Cl-rich fluids is not well constrained. They may have been produced during the late stages of magmatic crystallization, but further study is required.

TABLE OF CONTENTS

1. Introduction 4
2. Objectives and deliverables 4
3. Location 6
4. Regional geology 6
5. Sampling 8
6. Methods 8
7. Results
    7.1. Mineralogy of the Bégin-Lamarche deposit 12
    7.2. F and Cl contents of apatite 16
8. Discussion 16
9. Conclusions 20
10. References 21

1. Introduction

Chlorine (Cl) is a common minor or trace element in apatite or phosphatic ore and is corrosive to the equipment used for producing phosphoric acid from apatite concentrate (Chandra et al., 2017; Schorr and Valdez, 2017). Because Cl cannot be extracted from apatite prior to the production of phosphoric acid, ore containing low Cl contents is preferred (ca. < 500 ppm; Schorr et al., 2010). A blending of high-Cl apatite with low-Cl apatite before processing is also an option (Banerjee, 2023). Thus, understanding the distribution of Cl contents in phosphatic ores is critical for assessing the deposit's economic feasibility.

The purpose of this report is to characterize and investigate the genesis of phosphate layers with variable Cl contents (i.e., whole-rock Cl contents of 0.07-1.01 wt.%) from First Phosphate's Bégin-Lamarche property. The Bégin-Lamarche property is part of the Lac-Saint-Jean Anorthosite (LSJA) Complex in Quebec, Canada (Fig. 1A).

2. Objectives and deliverables

A recent drilling program by First Phosphate reveals that mafic rocks from the Bégin-Lamarche property contain multiple cumulate layers of phosphatic ores. Whole rock analysis of selected drill cores indicates that phosphatic ore horizons contain variable Cl contents (<600 to 10100 ppm; Table 1).

The detailed geological nature of the LSJA in the Bégin-Lamarche area is unknown. The primary objective of this study is to provide preliminary mineralogical and chemical data from 28 samples collected from 9 drill cores containing high (n=15) and low Cl (n=13) contents. Key deliverables include:

1) Petrographic thin-section investigation of phosphate-rich layers with both high and low whole-rock Cl contents to identify primary mineral assemblages.

2) Determination of modal abundances of major minerals using scanning electron microscope (SEM) based mineral liberation analysis (MLA).

3) Results of electron probe microanalysis (EPMA) of apatite and associated minerals for F and Cl concentrations.

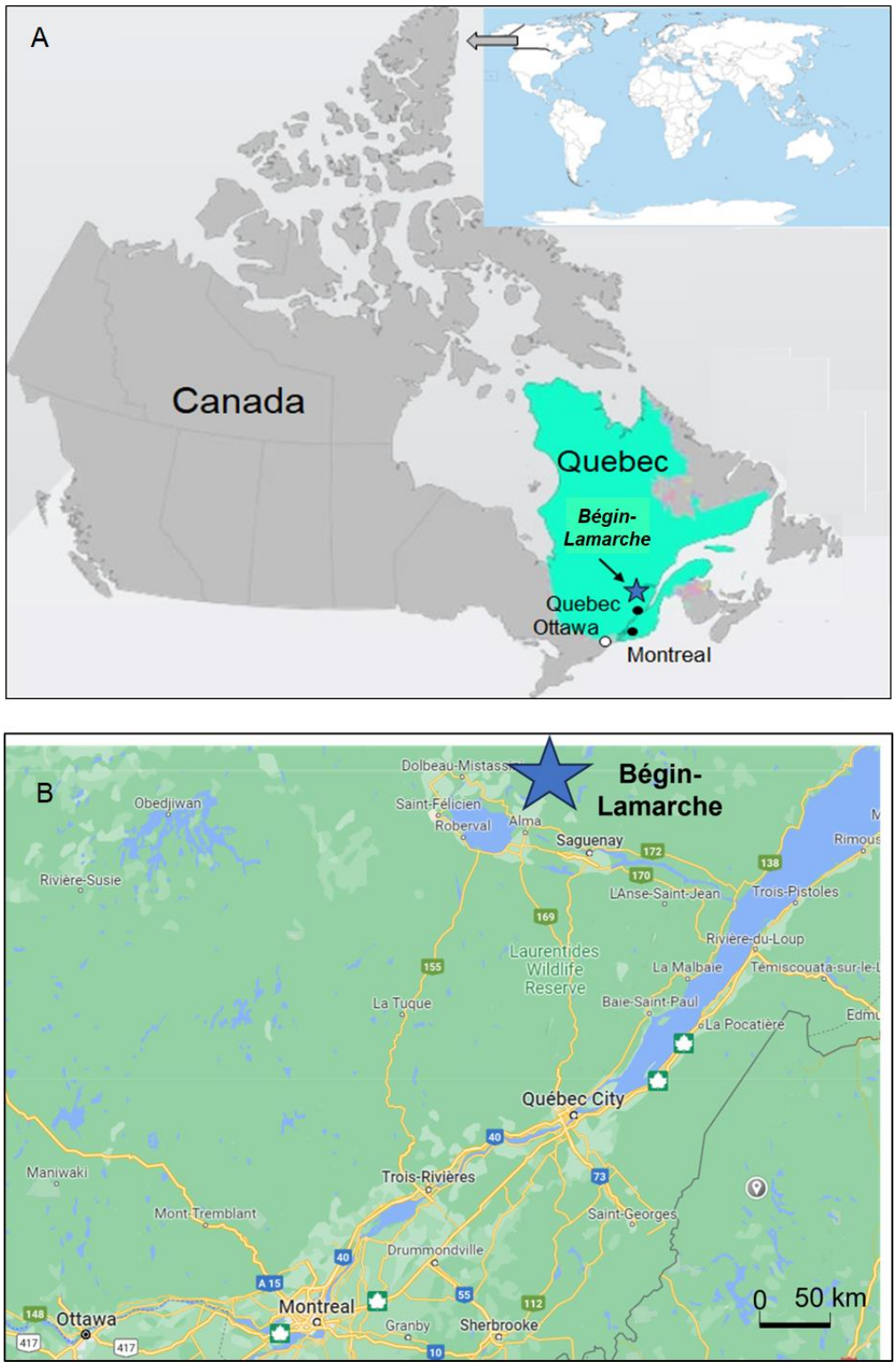

Fig 1. Location map (A and B) showing the Bégin-Lamarche property of First Phosphate Corp., Quebec, Canada.

3. Location

First Phosphate's Bégin-Lamarche property is located ~270 km north of Québec City, Quebec, Canada, and ~ 75 km southwest of Port Saguenay (Fig. 1B). The property is part of the LSJA Complex (Fig. 2), which is the world's largest anorthosite complex (Higgins et al., 2002; Grant, 2020).

The anorthosite-hosted phosphatic ore of the LSJA Complex is unique because most of the igneous phosphate ore in the world is produced from carbonatites and associated silica-deficient rocks in Russia, Brazil, and South Africa (Pufahl and Groat, 2017; El Bamiki et al., 2021; Jasinski, 2022).

4. Regional geology

The LSJA Complex occurs in the central part of the Grenville Structural Province (Fig. 2; Higgins and Breemen, 1992). The Grenville Structural Province is a ~1600 km long and ~350 km wide Mesoproterozoic orogenic belt along the southeastern margin of the Canadian Shield (Fig. 2). A prominent feature of the province is that it contains numerous anorthosite massifs and anorthosite-mangerite-charnockite-granite (AMCG) suites, including the LSJA Complex (Hébert et al., 2005).

The LSJA Complex consists of a complex assemblage of intrusive anorthosite plutons that are difficult to differentiate based on field relationships and mineralogy. Less abundant intrusive rocks include leuconorite, leucotroctolite, norite, olivine-bearing gabbro, gabbro, pyroxenite, peridotite, dunite, nelsonite, magnetitite, and rare charnockite–mangerite units (Hébert et al., 2005). All are composed of plagioclase with variable amounts of pyroxene and olivine (Higgins et al., 2002). Plagioclase is primarily andesine and labradorite (An_{45}- An_{60}; Higgins and Breemen, 1992).

The host rocks of the anorthosites of the LSJA Complex are the Chicoutimi Gneiss Complex (~1530 million years old), the Saguenay Gneiss Complex (~ 1506 million years old), the Hulot Complex (~1434 million years old), the Cap à l'Est Gneiss Complex, and the Cyriac Rapakivi Granite (~1393 to 1383 Ma million years old; Higgins and Breemen, 1996; Hébert et al., 2005).

The anorthosites of the LSJA Complex are interpreted to have intruded in multiple phases over ~170 million years starting at 1160 million years ago (Higgins et al., 2002). The complex defines three periods of magmatism recording a complex and protracted emplacement history. The first period occurred between 1160 and 1140 million years ago. The second was from 1082 to 1050 million years ago, and the third was between 1020 and 1000 million years ago (Higgins and Breemen, 1996). An accurate emplacement age for First Phosphate's Bégin-Lamarche deposit has not been determined.

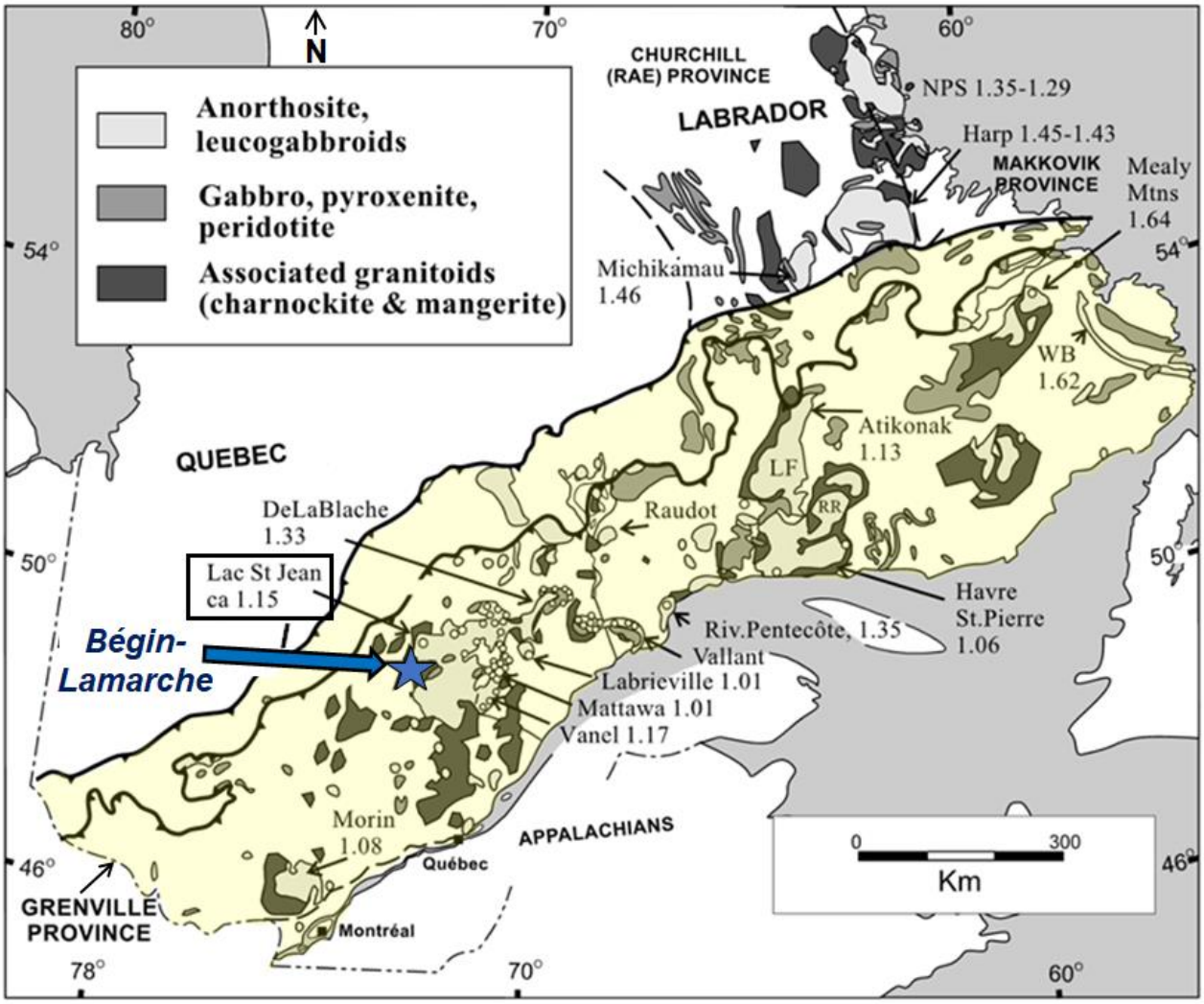

Fig. 2. Location map showing the Lac-Saint-Jean Anorthosite (LSJA) Complex, Bégin-Lamarche property of First Phosphate Corp., and other anorthosite bodies within the Grenville Province of Canada. The ages of the anorthosite bodies are also shown (in billion years). WB=White Bear Arm anorthosite, LF=Lac Fournier lobe, RR=riviere Romaine lobe (modified after Bedard, 2009; Higgins et al., 2002).

5. Sampling

Samples with high (700-10100 ppm of Cl) and low (≤ 600 ppm of Cl) whole-rock Cl contents were collected from drill holes from the north and south zones of the property (Fig. 3 and Table 1). A total of 28 core samples were collected from 9 drill holes; BL-23-01 (n=2), BL-23-03 (n=2), BL-23-06 (n=4), BL-23-10 (n=1), BL-23-12 (n=4), and BL-23-13 (n=4), BL-23-14 (n=4), BL-23-15 (n=4), and BL-23-18 (n=3; Table 1).

6. Methods

A total of 28 polished thin sections were prepared from selected areas of 28 quartered core samples. All polished thin sections were studied under transmitted and reflected light using a Nikon Eclipse LV 100N microscope for identifying minerals.

Eight polished thin sections were selected for more detailed analysis using SEM and EPMA. Six of these were from samples with high whole-rock Cl contents and two were from samples with low whole-rock Cl contents. All analyses were performed in the Queen's Facility for Isotope Research (QFIR), Queen's University, Canada.

This sub-suite of samples was analyzed with a FEI Quanta 650 FEG environmental scanning electron microscope (ESEM) utilizing mineral liberation analysis (MLA) to quantify mineral abundances. MLA was conducted under a low vacuum at a chamber pressure of 0.45torr. Energy-dispersive X-ray spectroscopy (EDS) was performed with two Bruker Nano Dual X-Flash detectors using an accelerating voltage of 25kV and a working distance of 12mm. Each sample was analyzed with a closely spaced grid of X-ray measurements overlain on a backscattered electron (BSE) image.

The *in-situ* chemical composition of minerals in this sub-suite was determined using a JEOL JXA-8230 electron microprobe. Electron probe microanalysis (EPMA) used an accelerating voltage of 15kV, a beam current of 20nA, a beam diameter of 5–10μm, and a counting time of 10s. Natural standards from the Smithsonian Institute were used for the analysis of all phases. The reported data represent an average of two or more analyses of each crystal and at least five crystals from different parts of each thin section. In the case of apatite, crystals with prismatic sections parallel to the c-crystallographic axis were identified under a petrographic microscope, and F and Cl contents were analyzed from those crystals. A total of 93 *in-situ* chemical analyses were performed on 39 apatite crystals from this sub-suite of eight samples. X-ray mapping of a single thin section of a sample containing high whole-rock Cl was further analyzed using complementary X-ray mapping. The X-ray mapping used an accelerating voltage of 15kV, a beam current of 200nA, and a dwell time of 60milliseconds.

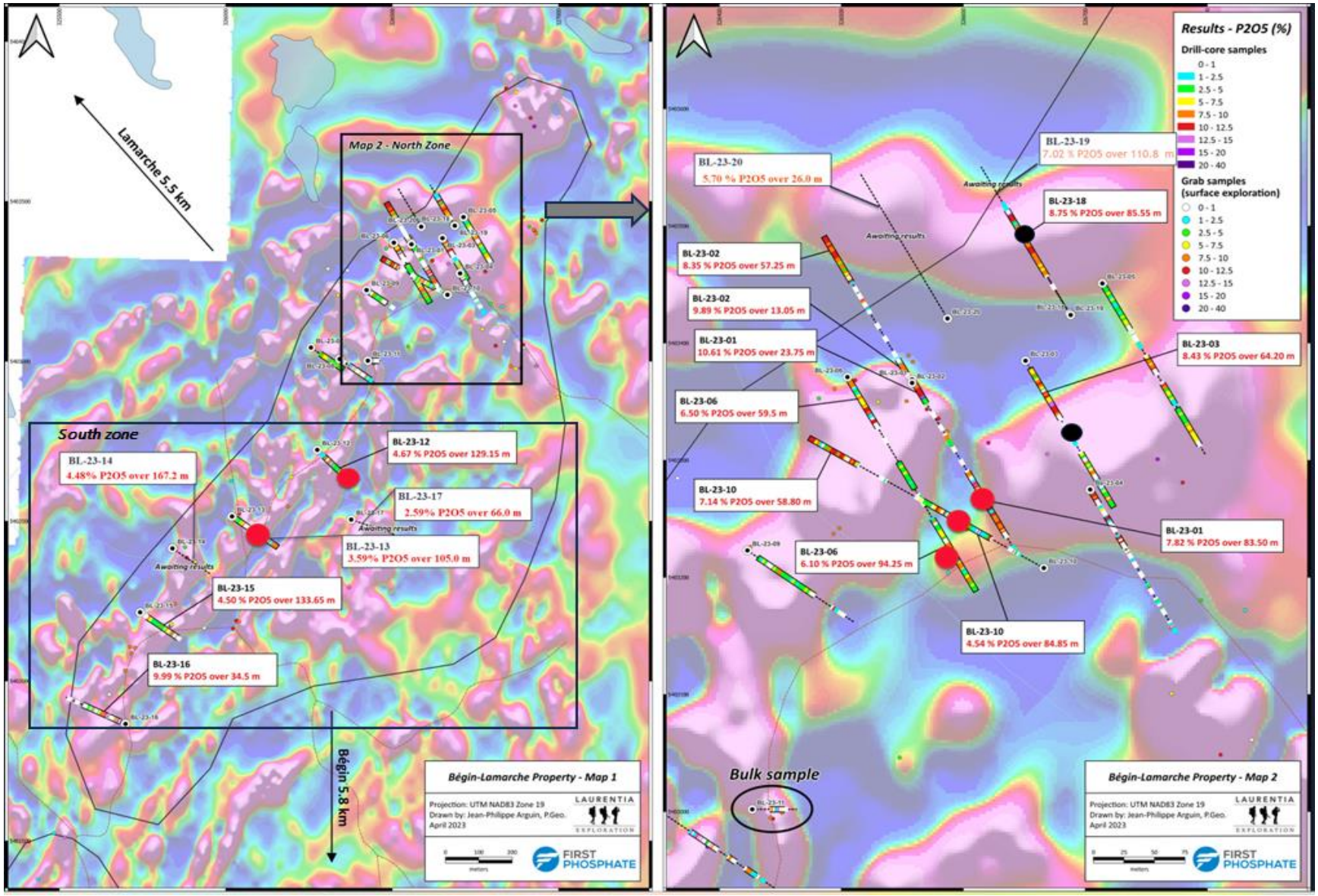

Fig. 3. Drill hole distributions within the Bégin-Lamarche property of First Phosphate Corp. Sampled drill cores are marked in red filled circles from which samples with high whole-rock Cl contents were collected and in black filled circles from which samples with low whole-rock Cl contents were collected (prepared by First Phosphate Corp.).

Table 1. Core samples with depths, average whole-rock P_2O_5, and Cl contents in the nine drill holes investigated in this study. Analysis types are also included.

			Whole-rock analysis				Analytical methods used in this study		
Ser. no	Zone	Bore hole	depth (m)	P_2O_5 (wt%)	Cl (wt%)		Petrographic thin section	SEM	EPMA
		Samples with high whole-rock Cl contents					***Samples with high whole-rock Cl contents***		
1	South zone	BL-23-12	147.1	12.35	0.1		✓		
2	South zone	BL-23-12	150.1	12.35	0.1		✓		
3	South zone	BL-23-12	152.7	12.35	0.13		✓	✓	✓
4	South zone	BL-23-12	155.8	12.35	0.07		✓		
5	South zone	BL-23-13	139.6	13.43	0.11		✓		
6	South zone	BL-23-13	142	13.43	0.12		✓		
7	South zone	BL-23-13	144.9	13.43	0.17		✓	✓	✓
8	South zone	BL-23-13	145.9	13.43	<0.01-0.17		✓		
9	North zone	BL-23-06	246.1	9.27	0.73		✓	✓	✓
10	North zone	BL-23-06	248.3	9.27	0.46		✓		
11	North zone	BL-23-06	250.3	9.27	0.46-0.81		✓		
12	North zone	BL-23-06	251.25	9.27	0.81		✓	✓	✓
13	North zone	BL-23-01	208.9	9.64-11.61	0.55-1.01		✓	✓	✓
14	North zone	BL-23-01	190.5	9.45-10.43	0.3-0.33		✓		
15	North zone	BL-23-10	122.85	11.46	0.09			✓	✓
		Samples with low whole-rock Cl contents					***Samples with low whole-rock Cl contents***		
16	South zone	BL-23-14	51	8.1	0.06		✓		
17	South zone	BL-23-14	54.3	8.1	0.06		✓		
18	South zone	BL-23-14	55	8.1	0.06		✓		
19	South zone	BL-23-14	56.8	8.1	0.06		✓		
20	South zone	BL-23-15	137.4	4.02	0.04		✓		
21	South zone	BL-23-15	139.3	4.02	0.04		✓		
22	South zone	BL-23-15	140.75	4.02	0.04		✓		
23	South zone	BL-23-15	142.6	4.02	0.04		✓		
24	North zone	BL-23-03	58.6	10.68	0.04		✓	✓	✓
25	North zone	BL-23-03	63	10.68	0.04		✓		
26	North zone	BL-23-18	108	9.07	0.04		✓		
27	North zone	BL-23-18	110	9.07	0.04		✓		
28	North zone	BL-23-18	114.2	9.07	0.04		✓	✓	✓
Total							***28***	***8***	***8***

Table 2. Major minerals and their modal abundances using MLA from the Bégin-Lamarche property of First Phosphate Corp. investigated in this study.

Ser. No	Zone	Bore hole	Depth (m)	Olivine	Serpentine	Orthopyroxene	Clinopyroxene	Amphibole (?)	Apatite	Magnetite	Ilmenite
Samples with high whole-rock Cl contents				modal (%)							
3	South zone	BL-23-12	152.7	15	8	<1	<1	<1	46	7	13
7	South zone	BL-23-13	144.9	8	25	<1	3	<1	31	8	9
9	North zone	BL-23-06	246.1	53	5	2	2	4.0	17	1	1
12	North zone	BL-23-06	251.25	11	21	<1	2	<1	31	6	15
13	North zone	BL-23-01	208.9	16	33	<1	4	<1	24	5	5
15	North zone	BL-23-10	122.85	8	25	<1	3	<1	31	8	9
Samples with low whole-rock Cl contents											
24	North zone	BL-23-03	58.6	17	2	11	1	1	23	10	15
28	North zone	BL-23-18	114.2	1	1	41	2	5	32	5	6
Plagioclase are present in all samples with low abundances (< 10%)											

7. Results

7.1. Mineralogy of the Bégin-Lamarche deposit

The ore mineral apatite from the Bégin-Lamarche property is hosted in peridotite. The major minerals forming this peridotite are olivine, orthopyroxene, clinopyroxene, plagioclase, amphibole, apatite, ilmenite, and magnetite. Biotite, Al-spinel, and sulfide mineral-pyrrhotite are present as accessory minerals (< 5 %). Common alteration minerals include serpentine and iddingsite. Cross-cutting calcite and serpentine veins are also common in some samples with high whole-rock Cl contents.

Based on the modal abundances of olivine, orthopyroxene, clinopyroxene, and plagioclase, the host rock, peridotite, can be more specifically characterized as an olivine gabbronorite. Estimated modal abundances of major minerals using MLA are provided in Table 2. The rocks show phaneritic texture. A brief description of the major minerals of the deposit is provided below.

Olivine (Mg_2SiO_4- Fe_2SiO_4) is the dominant mineral. Olivine crystals of the peridotite are subhedral in shape. The crystals range in size from ~0.2 to 3mm. Equant crystals of olivine are common (Fig. 4A and B). Olivine crystals are generally fractured. Fractures are filled with serpentine (Fig 4A). Many olivine crystals from samples with high whole-rock Cl contents are altered to iddingsite (Fig. 4B). Other alteration products of olivine include saponite and celadonite (Singh et al., 2023; Laverne et al., 2006), which occur in the samples with both high and low whole-rock Cl contents. Olivine has end-member compositions of forsterite (Mg_2SiO_4; 49.1-54.6mol%) and fayalite (Fe_2SiO_4; 45.4-50.9mol%). There is little variability in SiO_2 (34.4-35.2wt.%), MnO (0.56-0.59wt.%), and CaO (0.01-0.03wt.%) contents (Table 3).

Orthopyroxene ($Mg_2Si_2O_6$-$Fe_2Si_2O_6$) crystals are mostly subhedral in shape and equant in size (~0.5-2.0mm; Fig. 4C and D). They are associated with oxides (magnetite and ilmenite; Fig. 4C) and apatite (Fig. 4D) and are less altered than olivine.

Clinopyroxene ($(Ca,Mg,Fe)\ (Mg,Fe)Si_2O_6$) crystals are less abundant than orthopyroxene (Fig. 4D) and are also generally subhedral. Crystals range in size from ~0.5 to 2mm.

Plagioclase ($NaAlSi_3O_8$ – $CaAl_2Si_2O_8$) crystals are euhedral to subhedral (Fig. 4E and F) and mostly equant in size ranging from ~0.5 to 2mm. It has end-member compositions of anorthite (44.1-48.4mol.%), albite (51.5-52.7mol.%), and orthoclase (0.1-0.22mol.%). There is little variability in SiO_2 (55.0-55.8 wt.%) and Al_2O_3 (27.9-28.2 wt.%) contents (Table 3).

Amphibole ($(Na, K)_{0-1}\ (Na, Ca, Mg, Fe^{2+}, Mn^{2+}, Li)_2\ (Mg, Fe^{2+}, Fe^{3+}, Al, Mn, Zn, Cr, Ti, Li)_5\ (Si, Al)_8\ O_{22}\ (OH, F, Cl, O)_2$) crystals are identified under the optical microscope from the samples with low whole-rock Cl contents**.** The crystals are mostly subhedral in shape. The alterations of amphibole to clay minerals are also observed (Proust et al., 2006), which are mostly associated with plagioclase crystals (Fig. 4F).

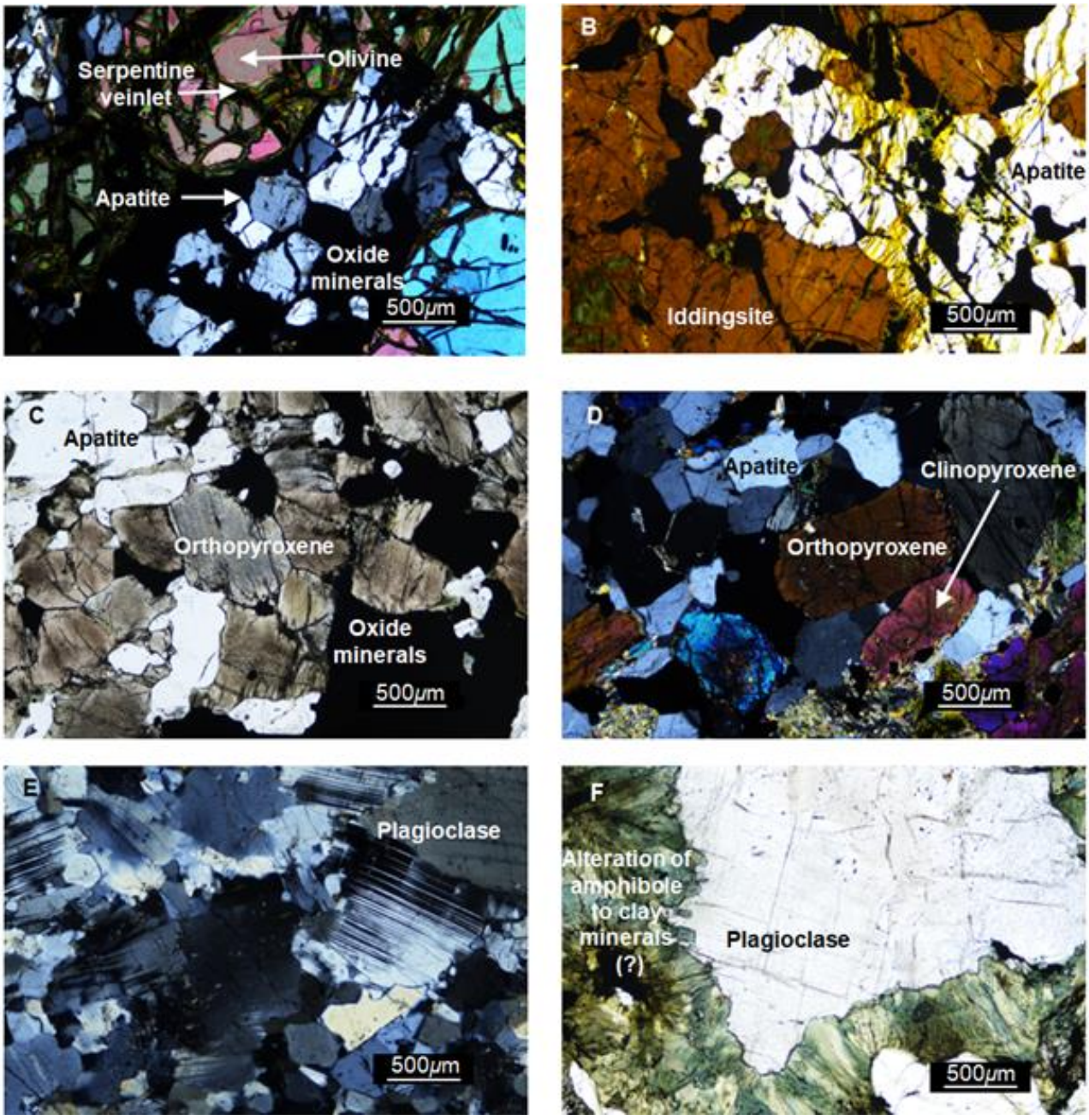

Fig. 4. Major silicate minerals present within the Bégin-Lamarche property of First Phosphate Corp. (A) Serpentine veinlets within olivine crystals (under cross-polarized light); (B) Iddingsite (altered products of olivine) associated with apatite (under plane-polarized light); (C) Orthopyroxene crystals associated with apatite crystals (under plane-polarized light); (D) Equant crystals of clinopyroxene and orthopyroxene (under cross-polarized light); (E) Equant crystals of plagioclase (under cross-polarized light); (F) Plagioclase crystal enclosed by amphibole crystals (under plane-polarized light).

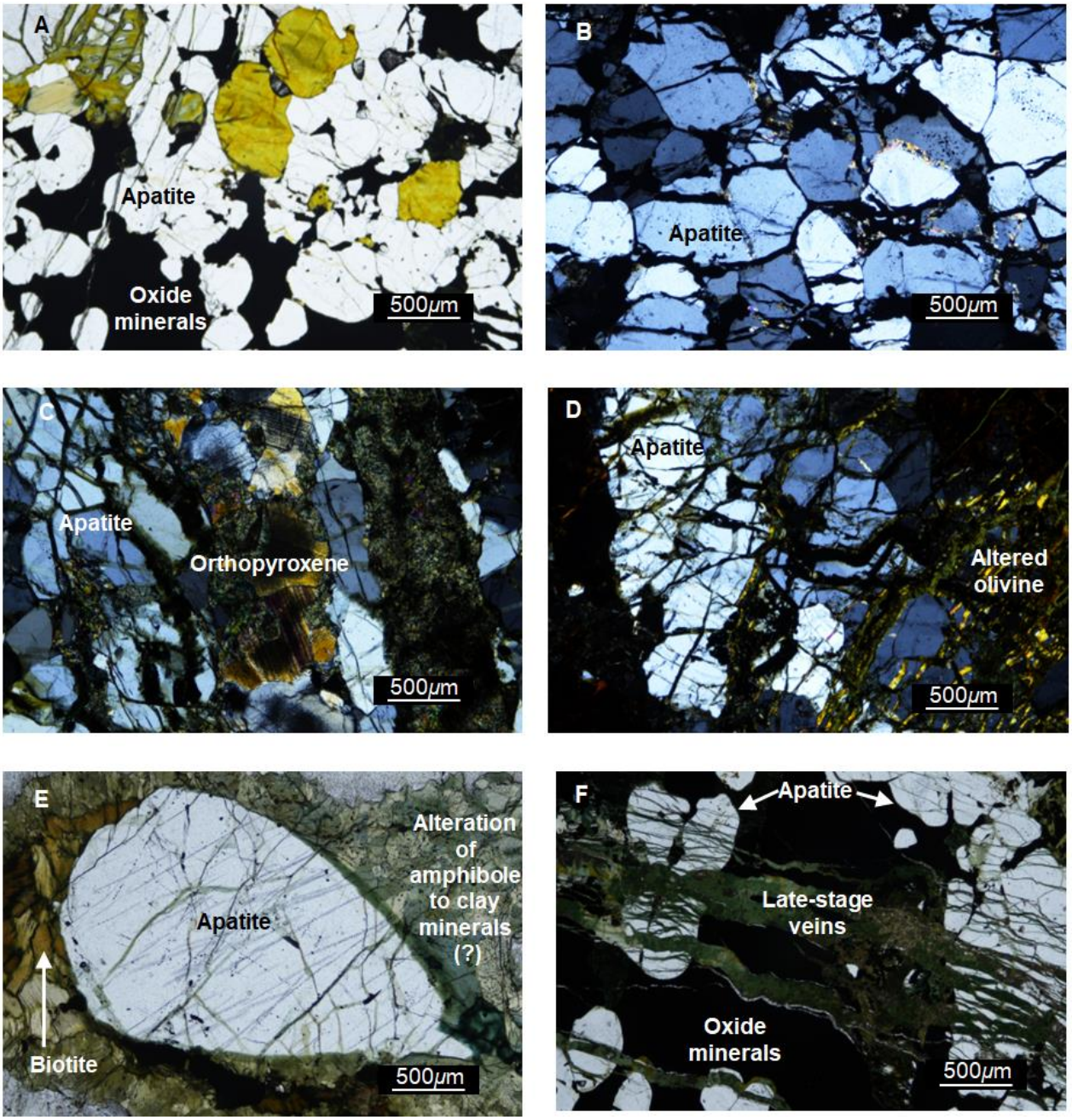

Fig. 5. Apatite (phosphatic ore) associated with different minerals within the Bégin-Lamarche property of First Phosphate Corp. (A) Apatite crystals associated with oxide minerals (under plane-polarized light); (B) Equant crystals of apatite associated with oxide minerals (under cross-polarized light); (C) Apatite crystals associated with orthopyroxene crystals (under cross-polarized light); (D) Apatite crystals associated with altered olivine (under cross-polarized light); (E) Apatite crystal enveloped by amphibole and biotite crystals (under plane-polarized light); (F) Late-stage veins cut through apatite crystals (under plane-polarized light).

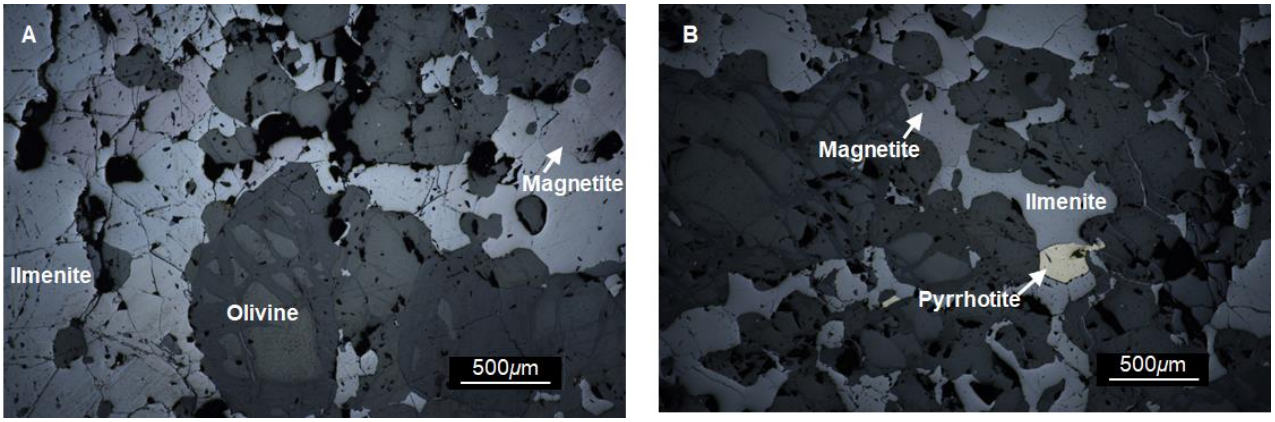

Fig. 6. Major oxide minerals from the Bégin-Lamarche property of First Phosphate Corp (under reflected light). (A) Magnetite and ilmenite crystals associated with serpentinized olivine crystals; (B) Pyrrhotite crystal (present as an accessory phase) associated with magnetite and ilmenite crystals.

Apatite ($Ca_5(PO_4)_3F$) mostly occurs as individual crystals associated with oxide minerals, orthopyroxene, olivine, and amphibole (Fig. 5A-F). Inclusions of apatite within olivine and orthopyroxene occur locally. Apatite crystals are euhedral to subhedral in shape and range in size from ~0.3 to 3mm. Late-stage veinlets of serpentine cross-cutting apatite are common in the peridodite (Fig. 5F). Apatite crystals have narrow ranges of CaO (54.8-55.4 wt.%) and P_2O_5 (41.8-42.4 wt.%) concentrations. The SiO_2 (≤0.04 wt.%), MnO (0.05-0.16 wt.%), MgO (0.04-0.15 wt.%), and FeO (0.14-0.31 wt.%) contents are low (Table 3). The F (2.63-3.0 wt.%) contents are higher than Cl (660-860 ppm) and H_2O concentrations (0.34-0.53 wt.%; Table 3). Mole fraction values of fluorapatite (X^{Ap}_{FAp}) range from 0.71 to 0.80 (Table 3). The X^{Ap}_{FAp} values are calculated following the procedure described by Piccoli and Candela (2002).

Ilmenite ($FeTiO_3$) and magnetite (Fe_3O_4) are the two dominant oxide minerals. Both are euhedral to subhedral, ranging in size from ~0.2 to 1.5mm (Fig. 6A and B).

7.2. F and Cl contents of apatite

F contents of apatite range from 2.63 to 3.0 wt.% (Table 4). F values from samples with high and low whole-rock Cl contents overlap (Table 4).

Cl contents of apatite from samples with high whole-rock Cl contents (3, 7, 9, 12, 13, 15) range from 664 to 703 ppm, which are significantly lower than their whole-rock Cl contents (900-8100 ppm; Table 4 and Fig. 7). The Cl contents of apatite from the two samples (24, 28) with low whole-rock Cl contents are 623 and 863 ppm, which are higher than their whole-rock Cl contents (400 ppm; Table 4 and Fig. 7).

An X-ray map of Cl content in apatite and associated minerals in one sample (13) with high whole-rock Cl content shows that Cl contents of apatite crystals are lower than those of altered olivine and those with late-stage veinlets (Fig. 8).

8. Discussion

Results indicate that whole-rock Cl contents and Cl contents of individual apatite crystals are not equal. In other words, the whole-rock Cl content of a peridotite sample does not necessarily correlate to the Cl content of apatite crystals forming that layer. The highest Cl content of apatite (863 ppm) is reported from samples (24) with low whole-rock Cl contents (400 ppm; Fig. 7 and Table 4). The Cl contents of apatite crystals (≤ 703 ppm) from the samples with high whole-rock Cl contents (3, 7, 9, 12, 13, 15) are significantly lower than those of the whole-rock samples (900-8100 ppm). Therefore, whole-rock Cl content cannot be used to infer the Cl content of apatite crystals forming the rock.

Table 3. Ranges of chemical compositions of plagioclase, olivine, and apatite of peridotites from the Bégin-Lamarche property of First Phosphate Corp. analyzed by EPMA.

	Olivine	Plagioclase	Apatite
	(wt%)		
SiO_2	34.4-35.2	55.0-55.8	≤0.04
Al_2O_3	≤0.01	27.9-28.2	≤0.01
FeO	38.5-42.1	0.08-0.14	0.14-0.31
MnO	0.56-0.59	n.a	0.05-0.16
MgO	22.8-26.0	n.a	0.04-0.15
CaO	0.01-0.03	9.70-9.95	54.8-55.4
Na_2O	n.a	5.84-6.0	0.02-0.08
K_2O	n.a	0.02-0.04	n.a
P_2O_5	n.a	n.a	41.8-42.4
F	n.a	n.a	2.63-3.00 (26300-30000 ppm)
Cl	n.a	n.a	0.07-0.9 (660-860 ppm)
H_2O	n.a	n.a	0.34-0.53
X^{Ap}_{FAp} (mole fraction of fluorapatite)	-	-	0.71-0.80
End members	$Fo_{49.1\text{-}54.6}$ $Fy_{45.4\text{-}50.9}$	$An_{44.1\text{-}48.4}$ $Ab_{51.5\text{-}52.7}$ $Or_{0.10\text{-}.22}$	-
Abbreviations: n.a: not analyzed, Fo: forsterite, Fy: fayalite, An: anorthite, Ab: albite, Or: orthoclase			

Table 4. Average F and Cl contents (±1σ) of apatite from selected samples from the Bégin-Lamarche property of First Phosphate Corp. Cl contents of whole rocks are also included.

Ser. No	Zone	Bore hole	depth (m)	F (wt%)	Cl (wt%)	Cl (ppm)	Whole rock Cl (ppm)
Samples with high whole-rock Cl contents							
3	South zone	BL-23-12	152.7	2.63±0.18	0.07±0.003	674±30	1300
7	South zone	BL-23-13	144.9	2.75±0.13	0.07±0.004	703±40	1700
9	North zone	BL-23-06	246.1	2.77±0.17	0.07±0.013	666±130	7300
12	North zone	BL-23-06	251.25	2.94±0.21	0.07±0.004	657±40	8100
13	North zone	BL-23-01	208.9	2.66±0.13	0.07±0.004	703±40	7800 (avg. of 5500 and 10100 ppm)
15	North zone	BL-23-10	122.85	2.92±0.15	0.07±0.006	664±60	900
Samples with low whole-rock Cl contents							
24	North zone	BL-23-03	58.6	2.77±0.20	0.09±0.021	863±210	400
28	North zone	BL-23-18	114.2	3.00±0.23	0.06±0.009	623±90	400

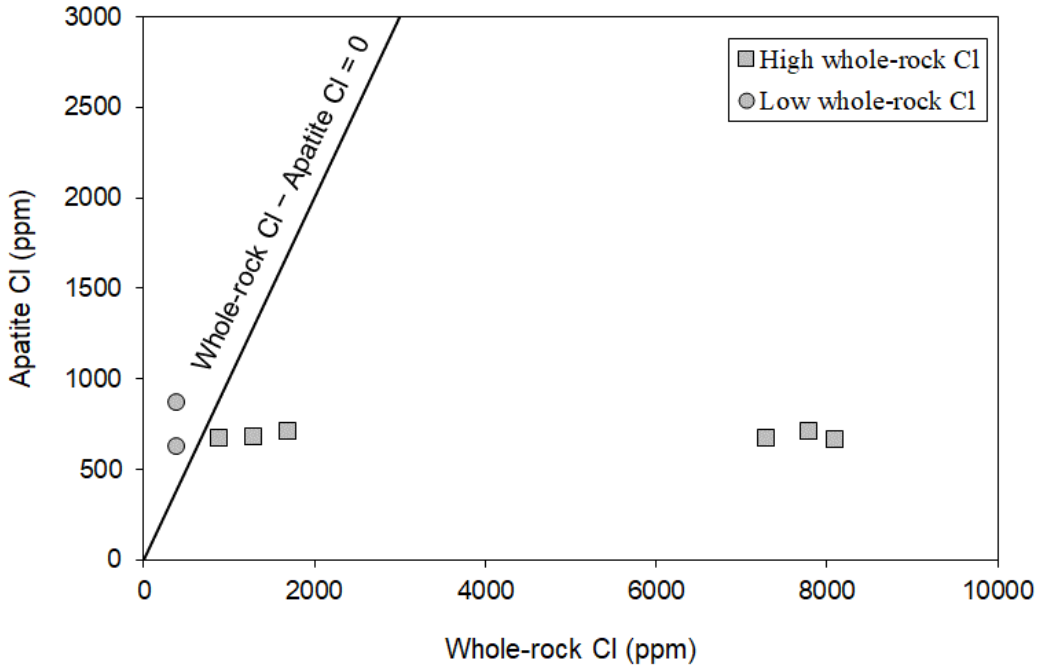

Fig. 7. Relationships of Cl contents of apatite and whole rock from the Bégin-Lamarche property of First Phosphate Corp.

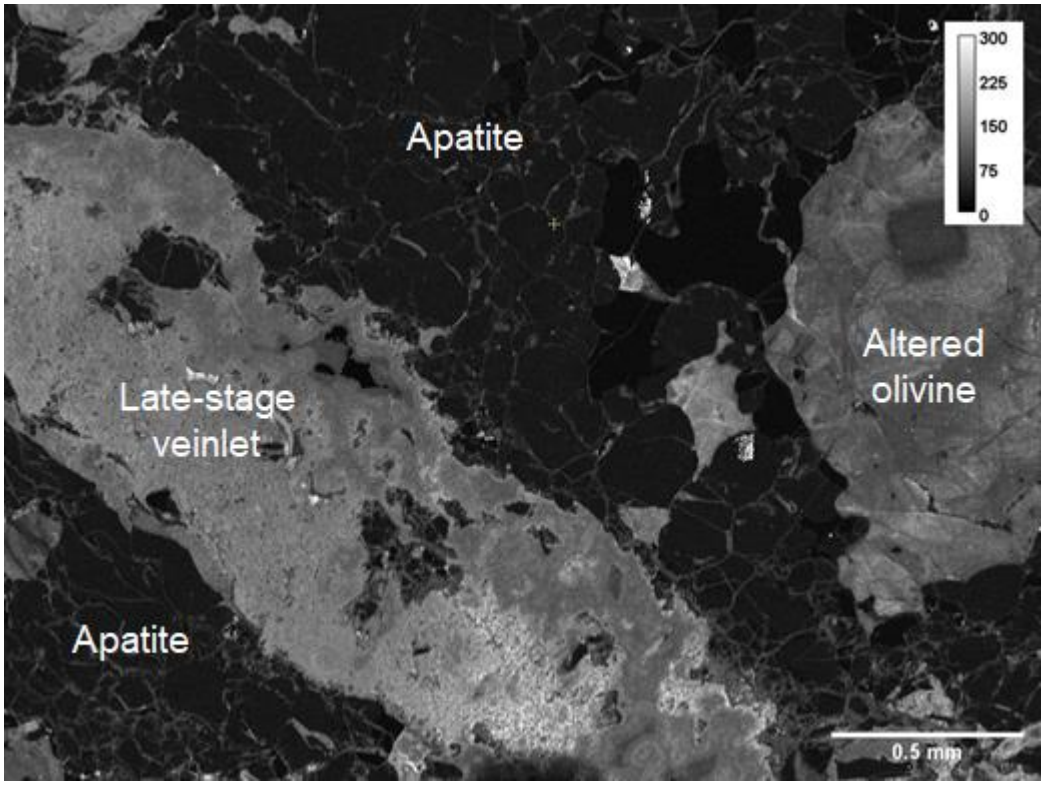

Fig. 8. X-ray map showing relative distributions of Cl in apatite and associated minerals from a sample (13) with high whole-rock Cl content. The greyscale (0-300) intensities indicate relative concentrations of Cl. Dark and light colours represent areas with relatively low and high Cl contents, respectively.

In general, samples with high whole-rock Cl contents (3, 7, 9, 12, 13, 15) show extensive alteration of olivine, i.e., the formation of iddingsite and dominance of serpentine veins or veinlets. Furthermore, X-ray mapping shows that altered olivine and late-stage veinlets contain higher Cl contents than that of the associated apatite crystals (Fig. 8). This style of alteration is interpreted to have been associated with late-stage brittle deformation and interaction with fluids containing high Cl concentrations. Further investigation is required to determine the source and timing of these fluids.

9. Conclusions

5. The Cl content of apatite crystals (≤703 ppm with one sample of 863 ppm) from a limited number of samples (n=8) suggests that the Cl contents of apatite or phosphatic cumulate layers of the deposit are low.
6. Whole-rock Cl content is not related to the Cl content of individual apatite crystals within the peridotite. The highest measured Cl concentration in apatite (863 ppm) is reported from a sample (24) with low whole-rock Cl content.
7. The Cl-enriched alteration minerals are iddingsite, and serpentine, which are associated with altered olivine and cross-cutting (serpentine) veins. This mineral assemblage was produced by the interaction with late-stage Cl-rich fluids and is responsible for the anomalously high Cl contents of some phosphatic cumulate layers.
8. The timing of the evolution of these Cl-rich fluids is not well constrained. They may have been produced during the late stages of magmatic crystallization, but further study is required.

10. References

Banerjee, S. (2022). Characterization of First Phosphate's Lac à l'Orignal phosphate deposit, Lac-Saint-Jean Anorthosite (LSJA) Complex, Quebec, Canada: Implications for supplying lithium ferro (Iron) phosphate (LFP) Batteries. (Technical report produced for First Phosphate Corp.) 56 pages.

Bédard, J.H. (2009). Parental magmas of Grenville province massif-type anorthosites, and conjectures about why massif anorthosites are restricted to the Proterozoic. Transactions of the Royal Society of Edinburgh 100, 77–103.

Chandra, K., Mahanti, A., Kain, V., Kumar, B.S., Kumar, N., and Gautam, V. (2017). Failure cases related to material issues in wet-process phosphoric acid plant. Engineering Failure Analysis, 79, 642-655.

El Bamiki, R., Raji, O., Ouabid, M., Elghali, A., Khadiri Yazami, O., and Bodinier, J. L. (2021). Phosphate Rocks: A Review of Sedimentary and Igneous Occurrences in Morocco. Minerals, 11(10), 1137.

Grant, M. (2020). Formation of Magmatic Fe-Ti-VP Deposits Within the Lac St. Jean Area Saguenay, Québec, Canada: Insights from Trace Element Composition of Fe-Oxides and Apatite (M.Sc dissertation, Université d'Ottawa/University of Ottawa).

Hébert, C., Cadieux, A. M., and van Breemen, O. (2005). Temporal evolution and nature of Ti–Fe–P mineralization in the anorthosite–mangerite–charnockite–granite (AMCG) suites of the south-central Grenville Province, Saguenay–Lac St. Jean area, Québec, Canada. Canadian Journal of Earth Sciences 42, 1865–80.

Higgins, M. D., Ider, M., and van Breemen, O. (2002). U–Pb ages of plutonism, wollastonite formation, and deformation in the central part of the Lac-Saint-Jean anorthosite suite. Canadian Journal of Earth Sciences 39, 1093–105.

Higgins, M. D., Ider, M., and van Breemen, O. (2002). U–Pb ages of plutonism, wollastonite formation, and deformation in the central part of the Lac-Saint-Jean anorthosite suite. Canadian Journal of Earth Sciences 39, 1093–105.

Higgins, M.D., and van Breemen, O. (1992). The age of the Lac-Saint-Jean Anorthosite Complex and associated mafic rocks, Grenville Province, Canada. Canadian Journal of Earth Sciences 29, 1412–1423.

Higgins, M.D., and van Breemen, O. (1996). Three generations of Anorthosite–Mangerite–Charnockite–Granite magmatism, contact metamorphism and tectonism in the Saguenay-Lac-St-Jean region, Grenville Province, Canada. Precambrian Research 79, 347–362.

Jasinski, S.M. (2022). Mineral commodity summary: phosphate rock. In: U.S. Geological Survey (2 p.).

Laverne, C., Grauby, O., Alt, J. C., and Bohn, M. (2006). Hydroschorlomite in altered basalts from Hole 1256D, ODP Leg 206: The transition from low-temperature to hydrothermal alteration. Geochemistry, Geophysics, Geosystems, 7(10).

Piccoli, P.M., and Candela, P.A. (2002). Apatite in igneous systems. Reviews in Mineralogy and Geochemistry, 48(1), 255-292.

Proust, D., Caillaud, J., and Fontaine, C. (2006). Clay minerals in early amphibole weathering: tri- to dioctahedral sequence as a function of crystallization sites in the amphibole. Clays and Clay Minerals, 54(3), 351-362.

Pufahl, P.K., and Groat, L.A. (2017). Sedimentary and igneous phosphate deposits: formation and exploration: an invited paper. Economic Geology, 112(3), 483-516.

Schorr, M., and Valdez, B. (2017). Phosphoric Acid Industry: Problems and Solutions. BoD – Books on Demand.

Schorr, M., Valdez, B., Zlatev, R., and Stoytcheva, M. (2010). Phosphate ore processing for phosphoric acid production: classical and novel technology. Mineral Processing and Extractive Metallurgy, 119(3), 125-129.

Singh, P., Banerjee, S., Choudhury, T. R., Bhattacharya, S., and Pande, K. (2023). Distinguishing celadonite from glauconite for environmental interpretations: a review. Journal of Palaeogeography, 12 (2), 179-194.